Supporting Information

Anchoring Ultra-small Molybdenum Oxide Species on Covalent Triazine Frameworks for Efficiently Electrochemical Nitrogen Fixation

Wenwen Lin,[ab] Teng Guo,[ab] Zihao Zhang,[a] Hao Chen,[c] Gaobo Lin,[ab] Yifeng Liu,[d] Siyu Yao,[a] Liang Wang,[a] Bolong Li, [ab] Jianghao Wang, [ab] Jie Fu*[ab] and Pingkai Ouyang†[a]

[a] Key Laboratory of Biomass Chemical Engineering of Ministry of Education, College of Chemical and Biological Engineering, Zhejiang University, Hangzhou 310027, China

[b] Institute of Zhejiang University-Quzhou, 99 Zheda Road, Quzhou, Zhejiang Province, 324000, China

[c] College of Chemistry and Chemical Engineering, Hunan University, Changsha 410082, China

[d] Key Lab of Applied Chemistry of Zhejiang Province, Department of Chemistry, Zhejiang University, Hangzhou 310028, China

*Corresponding author.

†Deceased 30 January 2023

E−mail address: jiefu@zju.edu.cn (*J. Fu*)

Experimental Procedures

Materials and Chemicals

2,6-dicyanopyridine (Aladdin, P138611, $C_7H_3N_3$, 97%), Zinc chloride (Aladdin, Z299383, $ZnCl_2$, 96%), acetone, acetonitrile (Aladdin, A104443, C_2H_3N, 99%), iodomethane (TCI, CH_3I, 99.5%), sodium molybdate dehydrate (Aladdin, S104867, $Na_2MoO_4{\cdot}2H_2O$, 99.0%), hydrochloric acid (SCR, HCl, analytically reagent), Isopropanol (Aladdin, I112016, C_3H_8O, 99.9%), potassium hydroxide (Aladdin, P112284, KOH, analytically reagent), hydrazine monohydrate (Aladdin, H104517,$N_2H_4{\cdot}H_2O$, >98.0%(T)), Nessler's reagent (Macklin, MFCD00049656, $K_2[HgI_4]$, analytically reagent), Potassium sodium tartrate tetrahydrate (Aladdin, P112611, $C_4H_4O_6KNa{\cdot}4H_2O$，99%), ammonium chloride (Sigma-Aldrich, 326372, NH_4Cl, 99.99%), ethyl alcohol (Macklin, E809061, C_2H_5OH, 99.7%), p-Dimethylaminobenzaldehyde (Macklin, P807320, $C_9H_{11}NO$, analytically reagent), carbon paper (HESEN, HCP120), 5% Nafion solution (Dupont), Nafion 211 membrane (Dupont), deionized water (Heal Force, 18.2 MΩ·cm) was used as the solvent, N_2 gas (99.99%), Ar gas (99.99%).

Synthesis of catalyst

Synthesis of CTF and Mo/CTF：CTF was fabricated in the sealed quartz tubes through ionothermal method using 2,6-dicyanopyridine (258 mg) as monomer and anhydrous ZnCl2 (2.72 g) as both solvent and catalyst based on the previous study[1]. After thermal treatment at 400 °C for 20 h and 600 °C for another 20 h, the resultant black powder

was ground and then washed three times with H_2O, HCl and acetone to remove $ZnCl_2$. The final product was obtained following a simple drying process. Mo/CTF was synthesized via an impregnation method with aqueous solution of Na_2MoO_4 as the Mo precursor. Briefly, Mo precursor was uniformly dropped into the CTF carrier and then stirred for 12 h. The resultant mixture was then dried overnight under reduced pressure at 55 °C followed by the calcination at 500 °C in H_2 atmosphere for 2 h to yield Mo/CTF.

Synthesis of CTF-I and Mo/CTF-I：In a typical experiment, 0.2 g CTF was mixed with 100 mL acetonitrile (CH_3CN) in a 250 mL three-necked Schlenk flask. 0.5 mL CH_3I was then added and refluxed at 80 °C for 24 h. CTF-I was thereafter obtained by the filtration, washing for three times with H_2O, CH_3CN, ethanol and acetone, as well as drying overnight at 50 °C. Mo/CTF-I was synthesized using the same method as Mo/CTF.

Cathode preparation

A 10 mg sample, 250 μL isopropanol and 50 μL of Nafion solution were dispersed in 750 μL absolute ethyl alcohol, and sonicated for 1 h to form a homogeneous ink. 100 μL of the dispersion was loaded onto a carbon paper electrode with area of 1x1 cm^2 and dried overnight at room temperature.

Calibration reference electrode

Ag/AgCl/saturated KCl was used as the reference electrode in all measurements. The

reference electrode was calibrated on a reversible hydrogen electrode (RHE). The calibration was performed in a high purity hydrogen saturated electrolyte with Pt foils as both the working electrode and the counter electrode in 0.5 M sulfuric acid electrolyte (pH=1). The OCPT was calibrated on a CHI660E electrochemical workstation for 30 min to obtain a stable horizontal line. The final stable potential value was considered to be the thermodynamic potential for the hydrogen electrode reactions. As a result, in 0.5 M sulfuric acid electrolyte (pH=1), E (RHE) = E (Ag/AgCl/saturated KCl) + 0.995 V in this work.

Electrochemical NRR measurements

The electrochemical experiments were carried out with an electrochemical workstation using a three-electrode configuration separated by a Nafion 211 membrane with a working electrode, a graphite rod counter electrode, and an Ag/AgCl (saturated KCl electrolyte) reference electrode. Before the NRR tests, the Nafion membrane was pretreated at 80 °C in a 5% H_2O_2 aqueous solution for 1 h and in ultrapure water for another 1 h.

For N_2 reduction experiments, a potentiostatic test was conducted in N_2-saturated 0.1 M KOH solution (50 mL), which was purged with N_2 for 30 min before the measurement. Pure N_2 (99.99% purity) was continuously fed to the cathodic compartment using properly positioned spargers. Ammonia synthesis was conducted under the potentiostatic mode (-0.3 V to -0.7 V vs. RHE) for 1 h at room temperature and atmospheric pressure. During ammonia synthesis, the cathode compartment was

supplied with N_2. For comparison, potentiostatic tests in Ar-saturated 0.1 M KOH solution and without potentiostatic tests in N_2-saturated 0.1 M KOH solution were also conducted in this work. All potentials were iR-compensated and converted to the RHE scale via calibration. Electrochemical impedance spectroscopy (EIS) was performed at open-circuit potential in the frequency range of 0.01 to 100000 Hz. To determine the electrochemical double layer capacitances (C_{dl}), cyclic voltammetry (CV) measurements were performed at various scan rates (from 10 to 100 mV s^{-1}) in the potential window between 0.1 V and 0.3 V vs. Ag/AgCl.

Determination of ammonia

In addition, the quantity of NH_3 formed was determined via a colorimetric method using Nessler's reagent. The calibration curve was plotted as follows: first, a series of reference solutions was prepared by pipetting suitable volumes of an ammonia-nitrogen 0.1 M KOH solution in colorimetric tubes. Second, fill up to the mark (10 mL) with a 0.1 M KOH solution. Third, 1 mL of 0.2 M potassium sodium tartrate ($KNaC_4H_4O_6$, chelating soluble metal ions) ultrapure water solution was added to each of the tubes and mixed thoroughly. Fourth, 1 mL of Nessler's reagent was added to each of the tubes and mixed thoroughly. Fifth, the solutions were allowed to sit for 40 minutes for color development. Sixth, background correction was performed with a blank solution, and the absorbance of the solutions was measured at 415 nm using a 10 mm glass cuvette.

Determination of hydrazine hydrate

The hydrazine present in the electrolyte was estimated by the method of Watt and Chrisp.[2] A mixture of para-(dimethylamino) benzaldehyde (5.99 g), HCI (concentrated, 30 mL) and ethanol (300 mL) was used as a color reagent. The calibration curve was plotted as follows: first, a series of reference solutions was prepared by pipetting suitable volumes of hydrazine hydrate-nitrogen 0.1 M KOH solution into colorimetric tubes. Second, 5 mL of 0.1 M KOH solution was used. Third, 5 mL of the above prepared color reagent was added and stirred for 10 min at room temperature. Fourth, the absorbance of the resulting solution was measured at 457 nm, and the yields of hydrazine were estimated from a standard curve using 5 mL of the residual electrolyte and 5 mL of the color reagent.

Faradaic efficiency

The Faradaic efficiency for the NRR was defined as the quantity of electric charge used for synthesizing ammonia divided by the total charge passed through the electrodes during electrolysis. The total amount of NH_3 produced was measured using the colorimetric methods. Assuming three electrons were needed to produce one molecule of NH_3, the Faradaic efficiency can be calculated as follows:

$$FE_{NH_3} = \frac{aF \times n_{NH_3}}{Q}$$

where a is the quantity of transferred electrons for producing NH_3, F is the Faraday constant, n_{NH3} is the molar mass of NH_3, and Q is the total quantity of the electric charge.

The rate of ammonia formation was calculated using the following equation:

$$Yield_{\left(\mu g\, h^{-1}\, mg_{cat.}^{-1}\right)} = \frac{c_{NH_3} \times V}{t \times m_{cat.}}$$

where c_{NH3} is the measured NH_3 concentration, V is the volume of the KOH electrolyte, t is the reaction time, and $m_{cat.}$ is the mass of catalyst.

Characterizations

X-ray diffraction (XRD) patterns were obtained by using a Bruker diffractometer with Cu Kα radiation (D8 Advance X-ray diffractometer, Cu Kα, λ= 1.5406 Å, 40 kV, and 40 mA). An X-ray photoelectron spectrometer (XPS; VG ESCALAB MKII instrument) with an Al Kα X-ray source was used to analyze the surface chemical properties of the samples. N_2 adsorption and desorption were measured using the Micromeritics ASAP2020. Specific surface area was calculated by the Brunauer–Emmett–Teller (BET) equation. The Mo content in the catalysts was determined by inductive coupled plasma optical emission spectrometry (ICP-OES) on Varian T30-ES. Field-emission scanning electron microscope (SEM; Hitachi New Generation SU8010), and a transmission electron microscope (TEM; JEOL, JEM-2010, 200 kV) equipped with energy dispersive X-ray spectroscopy (EDX) was used to observe the morphology and elemental composition of the materials. Scanning transmission electron microscopy (STEM) was performed on FEI Titan G2 80-200 ChemiSTEM. The Mo K-edge X-ray absorption near edge structure (XANES) spectra were collected at BL14W1 beamline at Shanghai Synchrotron Radiation Facility (SSRF) using QXAFS mode. The C and N K-edge XANES spectra were collected at BL08U1A beamline at SSRF. All spectra were processed using the Athena software within the Ifeffit package.

Results and Discussion

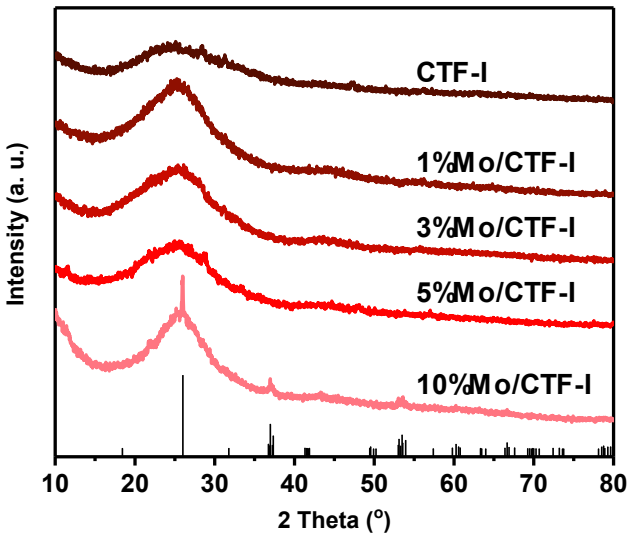

Figure S1. XRD patterns with different Mo loads.

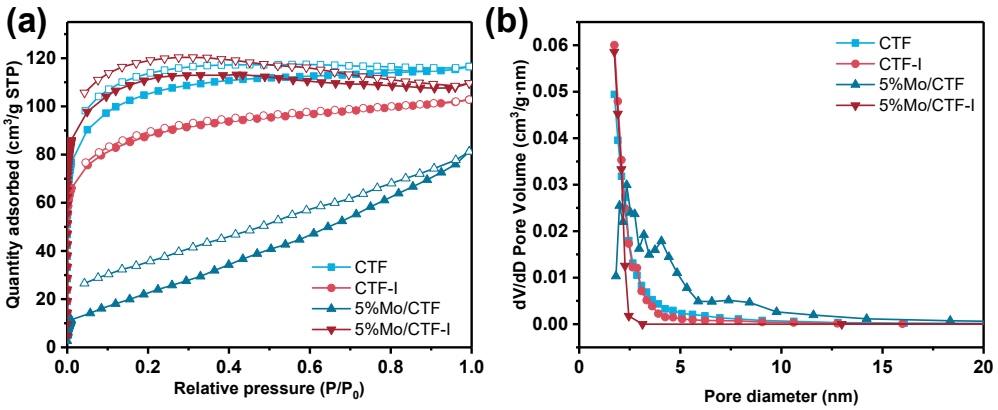

Figure S2. (a) N_2 adsorption−desorption isotherms of CTF, CTF-I, 5% Mo/CTF, and 5% Mo/CTF-I. (b) The pore size distribution of CTF, CTF-I, 5% Mo/CTF, and 5% Mo/CTF-I.

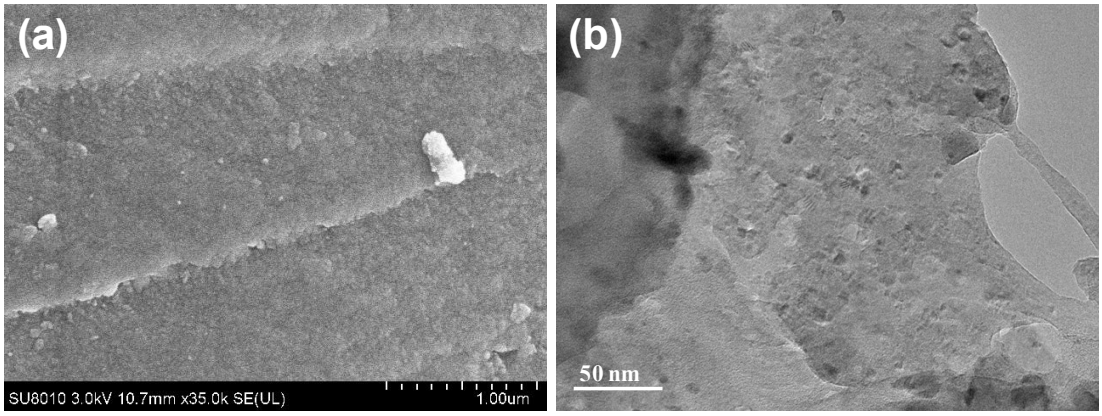

Figure S3. For CTF-I (a) SEM images. (b) TEM images.

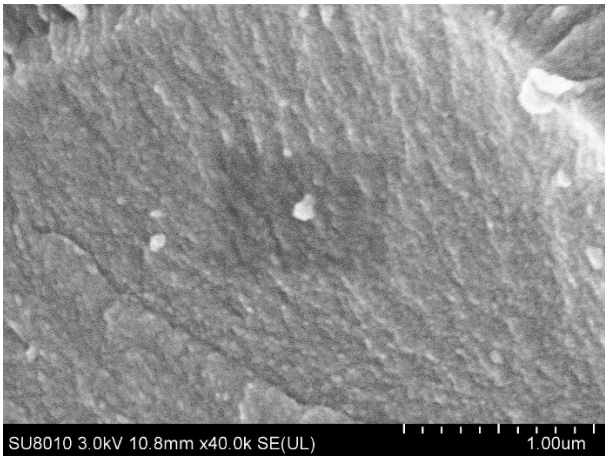

Figure S4. SEM image of 5%Mo/CTF-I.

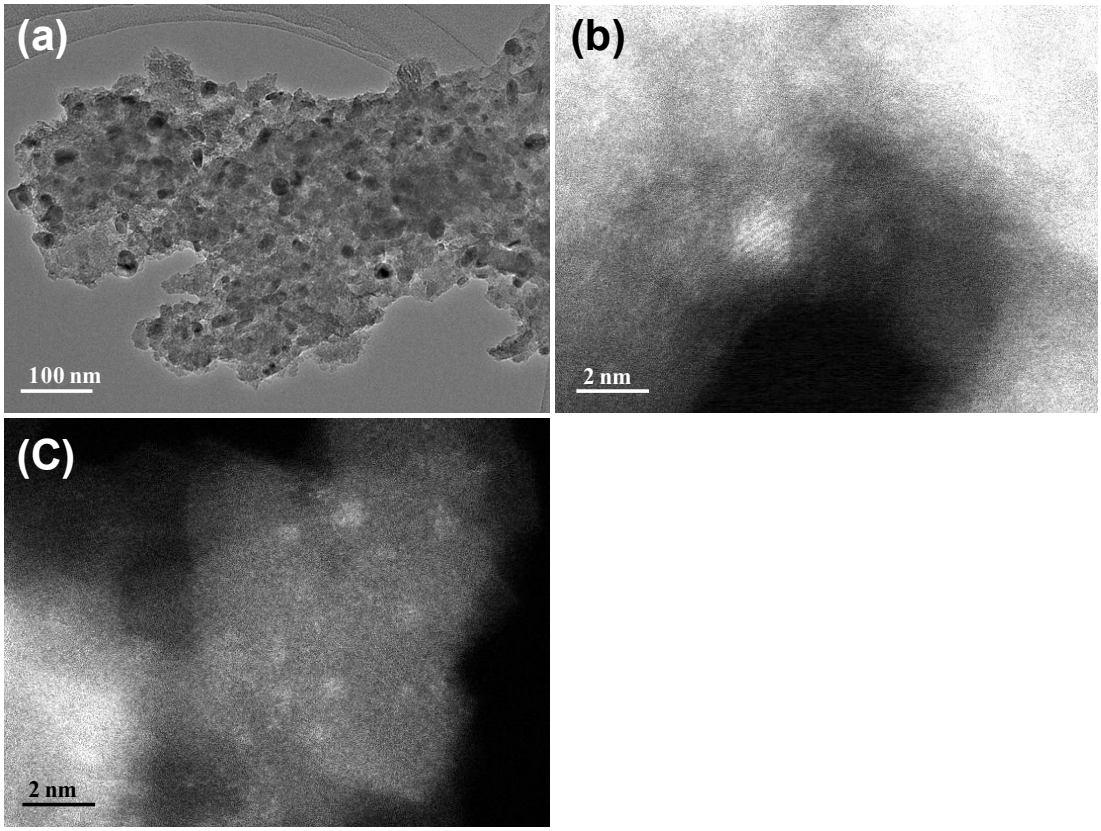

Figure S5. (a) TEM images for 5% Mo/CTF. (b, c) HAADF images of 5%Mo/CTF.

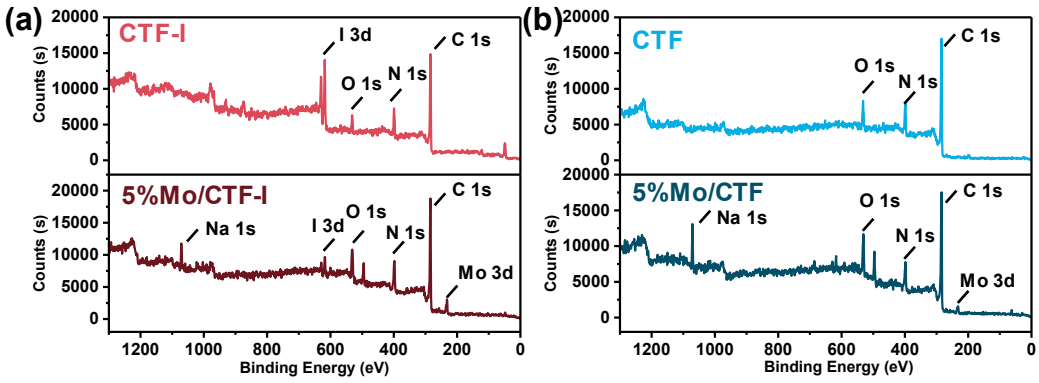

Figure S6. XPS spectra of (a) CTF-I and 5% Mo/CTF-I, (b) CTF and 5% Mo/CTF.

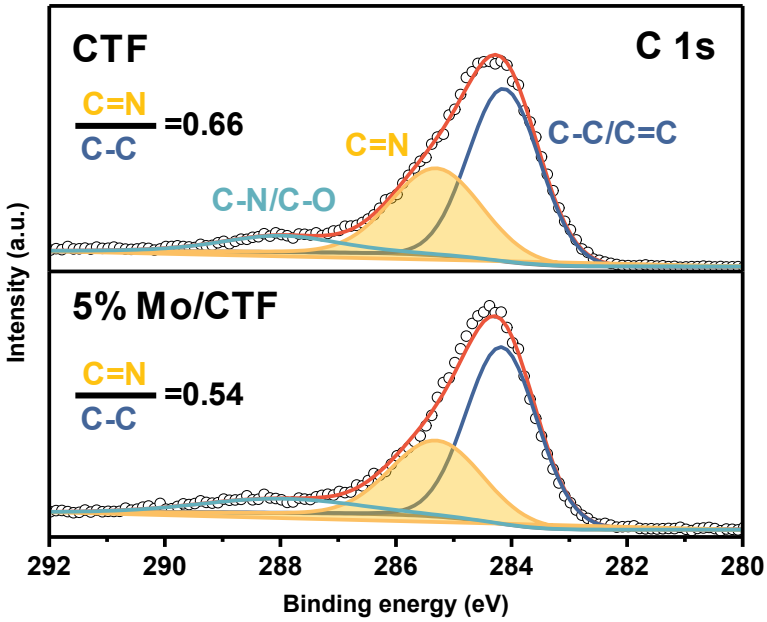

Figure S7. C 1s XPS spectra of CTF and 5% Mo/CTF.

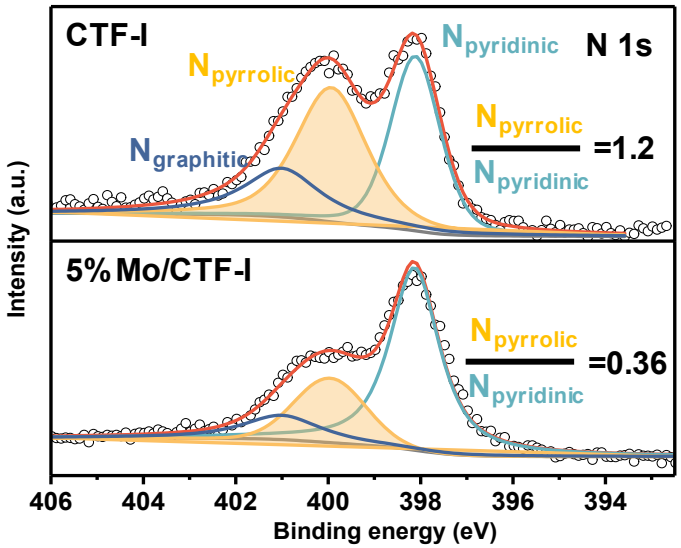

Figure S8. N 1s XPS spectra of CTF and 5% Mo/CTF.

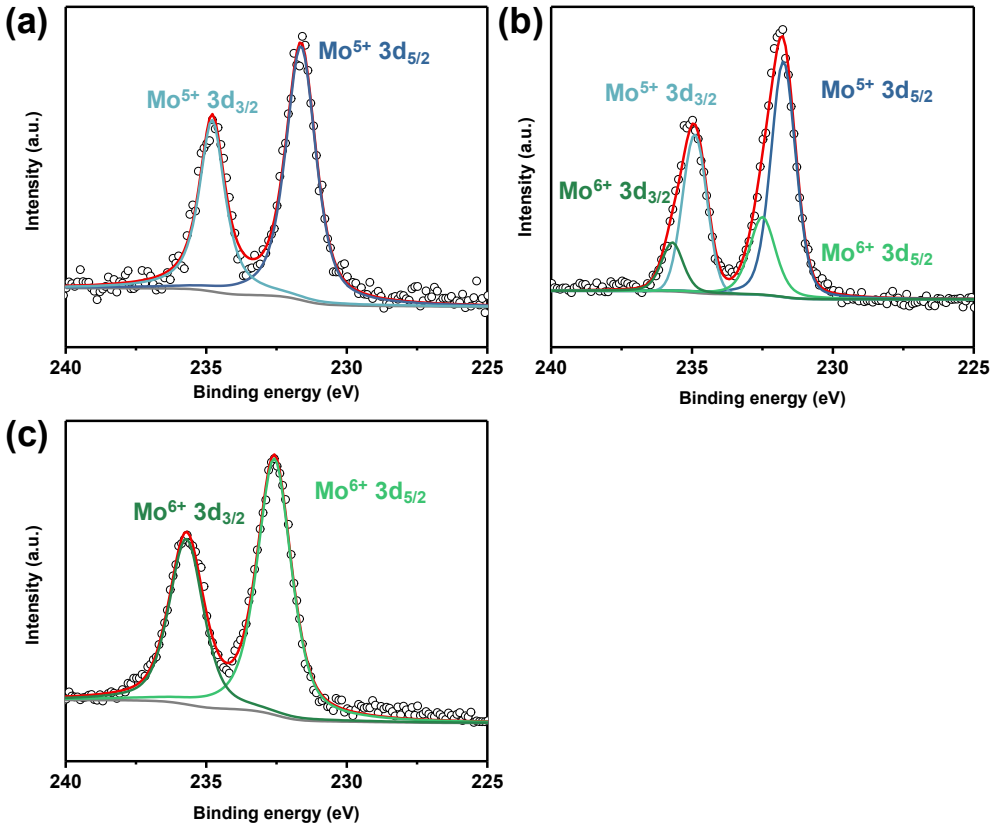

Figure S9. XPS spectra of the Mo 3d for (a) 5%Mo/CTF, (b) 5%Mo/AC, and (c) 5% Mo/CTF-I-unreduced.

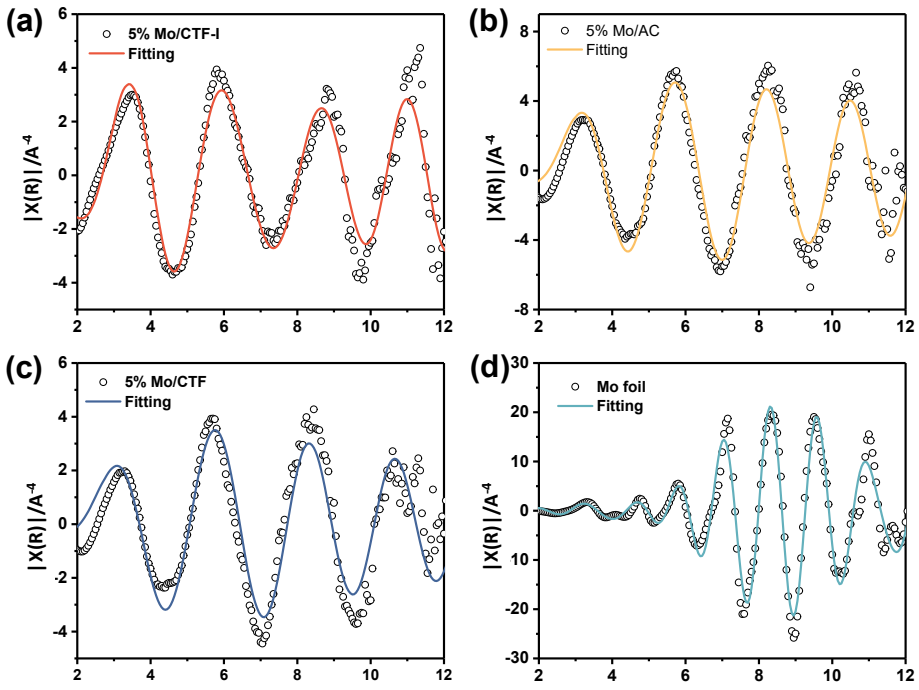

Figure S10. EXAFS fitting curve for Mo in (a) 5%Mo/CTF-I, (b) 5%Mo/AC, (c) 5% Mo/CTF, and (d) Mo foil.

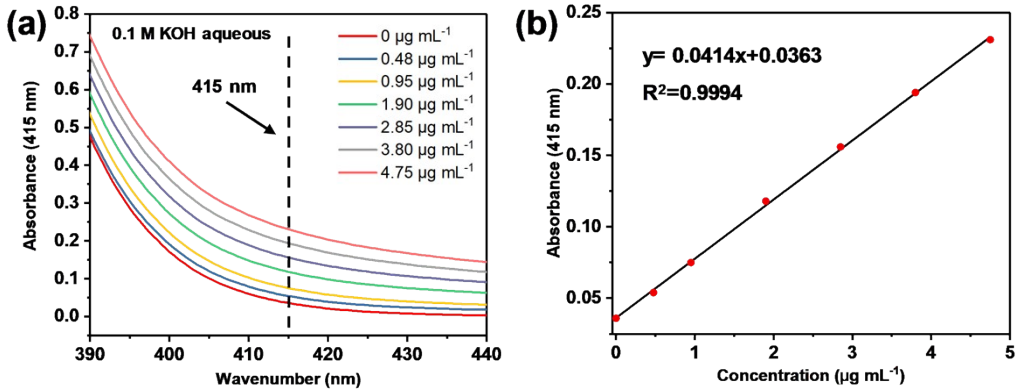

Figure S11. Calibration curve for colorimetric NH_3 assay using Nessler reagent. (a) UV-Vis curves of colorimetric NH_3 assays with NH^{4+} ions after incubated for 30 min at room temperature; (b) calibration curve used for estimation of NH_3 by NH^{4+} ion concentration. The absorbance at 415 nm was measured by UV-V is spectrophotometer, and the fitting curve shows good linear relation of absorbance with NH^{4+} ion concentration ($y=0.0414x+0.0363$, $R^2=0.9994$).

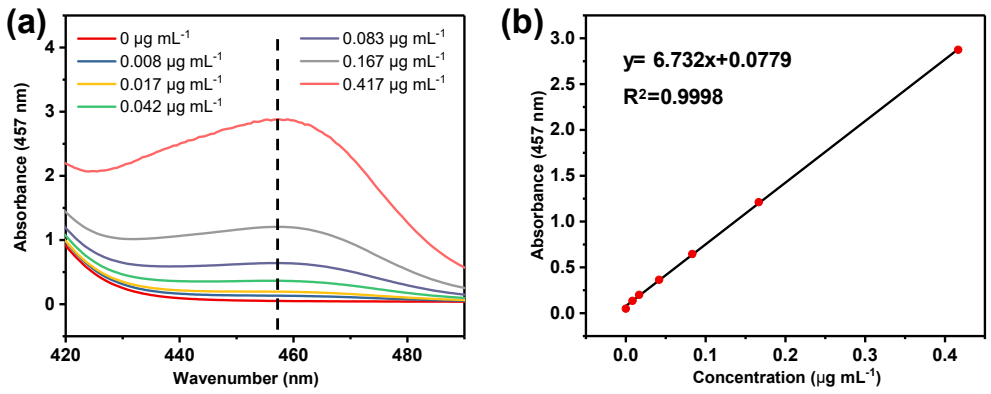

Figure S12. Absolute calibration of the Watt and Chrisp (para- dimethylamino-benzaldehyde) method for estimating $N_2H_4 \cdot H_2O$ concentration, using $N_2H_4 \cdot H_2O$ solutions of known concentration as standards. (a) UV-V is curves of various $N_2H_4 \cdot H_2O$ concentration after incubated for 10 min at room temperature; (b) calibration curve used for estimation of $N_2H_4 \cdot H_2O$ concentration. The absorbance at 457 nm was measured by UV-V is spectrophotometer, and the fitting curve shows good linear relation of absorbance with $N_2H_4 \cdot H_2O$ concentration (y=0.5693x+0.0167, R^2=0.9994) of three times independent calibration curves.

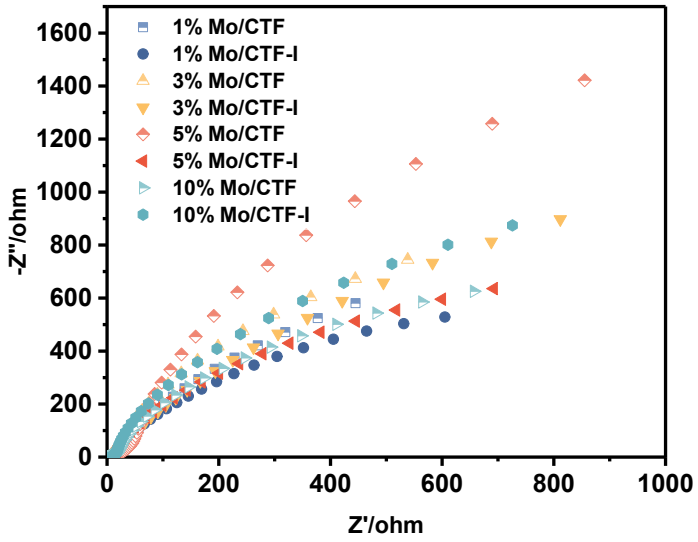

Figure S13. The electrochemical impedance spectra of CTF and CTF-I with different Mo load.

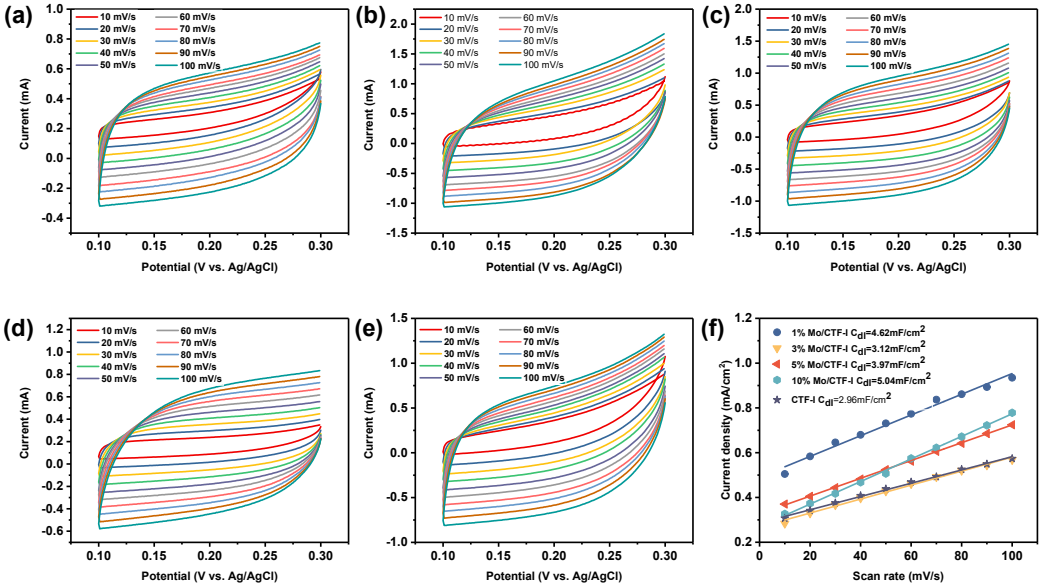

Figure S14. Cyclic voltammetry curves against different scan rates (a) CTF-I. (b) 1%Mo/CTF-I. (c) 3%Mo/CTF-I C. (d) 5%Mo/CTF-I. (e) 10%Mo/CTF-I. (f)The double-layer capacitance (Cdl) values.

Table S1. Specific surface area and pore volume of Mo/ CTF catalysts.

	S_{BET} m^2/g	S_{micro} m^2/g	$S_{external}$ m^2/g	V cm^3/g
CTF	376	244	132	0.18
CTF-I	312	186	126	0.16
5%Mo/ CTF-I	399	297	102	0.17
5%Mo/ CTF	127	74	53	0.12

Table S2. The mass fraction of Mo measured from ICP results.

Catalyst	Mo (wt.%)
5% Mo/CTF-I	5.61
5% Mo/CTF	4.75
10% Mo/CTF-I	8.66
10% Mo/CTF	2.48

Table S3. EXAFS fitting result of 5% Mo/CTF-I, 5% Mo/CTF, and 5% Mo/AC.

Mo S^2=0.8

	Mo-O			ΔE_0(eV)
	R(Å)	CN	δ	
5% Mo/CTF-I	1.71±0.02	2.67±0.22	0.002	8.15±2.95
5% Mo/CTF	1.72±0.01	2.98±0.27	0.003	5.51±3.00
5% Mo/AC	1.75±0.01	3.94±0.31	0.002	0.044±2.57

Table S4. Summary of the representative reports on NRR catalysts

Catalysts	Electrolyte	NH_3 Yield Rate	Faradaic Efficiency (%)	Potential (vs. RHE)	Ref.
(110)-oriented Mo nanofilm	0.5 M H_2SO_4	3.09×10^{-11} mol s^{-1} cm^{-2}	0.72	-0.49 V	3
MoS_2 nanosheet array	0.1 M Na_2SO_4	8.08×10^{-11} mol s^{-1} cm^{-1}	1.17	-0.5	4
Mo_2C/C	0.5 M Li_2SO_4	11.3 μg h_{-1} mg^{-1}_{Mo2C}	7.8	-0.3	5
defect-rich MoS_2 nanoflowers	0.1 M Na_2SO_4	29.28 μg h^{-1} $mg^{-1}_{cat.}$	8.34	-0.4	6
Co-doped MoS_2-x nanosheets	0.01 M H_2SO_4	0.63 mmol h^{-1} g^{-1}	>10	-0.3	7
FeS@MoS_2/CFC	0.1 M Na_2SO_4	8.45 μg h^{-1} cm^{-2}	2.96	-0.5	8
S-rich MoS_2 nanosheets	0.1 M Li_2SO_4	43.4 μg h^{-1} mg^{-1}_{MoS2}	9.81	-0.2	9
Fe-MoS_2 nanosheet	0.1 M KOH	12.5 μg h^{-1} cm^{-2}	10.8	-0.1	10
Mo_3Fe_3C	0.1 M Li_2SO_4	72.5 μg h^{-1} $mg^{-1}_{cat.}$	27	-0.2	11
1T''' MoS_2	0.1 M Na_2SO_4	9.24 μg h^{-1} mg^{-1}	13.4	-0.3	12
Mo_2C/NC	0.1 M Na_2SO_4	70.6 μmol h^{-1} $g^{-1}_{cat.}$	12.3	-0.2	13
NiO-NFs	0.1 M Na_2SO_4	16.16 μg h^{-1} $mg^{-1}_{cat.}$	9.17	-0.4	14
NiO NSs@CF	0.1 M Na_2SO_4	71.3 μg h^{-1} $mg^{-1}_{cat.}$	17.9	-0.5	15
5% Mo/CTF-I	0.1 M HCl	7.23 μg h^{-1} $mg^{-1}_{cat.}$	27.3	-0.405	This work

References

1. J. Roeser, K. Kailasam and A. Thomas, *CHEMSUSCHEM*, 2012, **5**, 1793-1799.
2. G. W. Watt and J. D. Chrisp, *ANALYTICAL CHEMISTRY*, 1952, **24**, 2006-2008.
3. D. S. Yang, T. Chen and Z. J. Wang, *JOURNAL OF MATERIALS CHEMISTRY A*, 2017, **5**, 18967-18971.
4. L. Zhang, X. Q. Ji, X. Ren, Y. J. Ma, X. F. Shi, Z. Q. Tian, A. M. Asiri, L. Chen, B. Tang and X. P. Sun, *ADVANCED MATERIALS*, 2018, **30**.
5. H. Cheng, L. X. Ding, G. F. Chen, L. L. Zhang, J. Xue and H. H. Wang, *ADVANCED MATERIALS*, 2018, **30**.
6. X. H. Li, T. S. Li, Y. J. Ma, Q. Wei, W. B. Qiu, H. R. Guo, X. F. Shi, P. Zhang, A. M. Asiri, L. Chen, B. Tang and X. P. Sun, *ADVANCED ENERGY MATERIALS*, 2018, **8**.
7. J. Zhang, X. Y. Tian, M. J. Liu, H. Guo, J. D. Zhou, Q. Y. Fang, Z. Liu, Q. Wu and J. Lou, *JOURNAL OF THE AMERICAN CHEMICAL SOCIETY*, 2019, **141**, 19269-19275.
8. Y. X. Guo, Z. Y. Yao, B. J. J. Timmer, X. Sheng, L. Z. Fan, Y. Y. Li, F. G. Zhang and L. C. Sun, *NANO ENERGY*, 2019, **62**, 282-288.
9. Y. Y. Liu, M. M. Han, Q. Z. Xiong, S. B. Zhang, C. J. Zhao, W. B. Gong, G. Z. Wang, H. M. Zhang and H. J. Zhao, *ADVANCED ENERGY MATERIALS*, 2019, **9**.
10. X. H. Zhao, X. Zhang, Z. M. Xue, W. J. Chen, Z. Zhou and T. C. Mu, *JOURNAL OF MATERIALS CHEMISTRY A*, 2019, **7**, 27417-27422.
11. B. H. Qin, Y. H. Li, Q. Zhang, G. X. Yang, H. Liang and F. Peng, *NANO ENERGY*, 2020, **68**.
12. G. X. Lin, Q. J. Ju, X. W. Guo, W. Zhao, S. Adimi, J. Y. Ye, Q. Y. Bi, J. C. Wang, M. H. Yang and F. Q. Huang, *ADVANCED MATERIALS*, 2021, **33**.
13. Y. Z. Zhang, J. Hu, C. X. Zhang, A. T. F. Cheung, Y. Zhang, L. F. Liu and M. K. H. Leung, *INTERNATIONAL JOURNAL OF HYDROGEN ENERGY*, 2021, **46**, 13011-13019.
14. M. Zhou, W. Xiong, H. Li, D. Zhang and Y. Lv, *Dalton Transactions*, 2021, **50**, 5835-5844.
15. W. Xiong, M. Zhou, X. Y. Huang, W. J. Yang, D. Zhang, Y. K. Lv and H. Li, *CHEMISTRY-A EUROPEAN JOURNAL*, 2022, **28,** e202200779.